Langmuir
Article
pubs.acs.org/Langmuir

Dispersions of Nanoclays of Different Shapes into Aqueous and Solid Biopolymeric Matrices. Extended Physicochemical Study

Giuseppe Cavallaro, Giuseppe Lazzara,* and Stefana Milioto

Dipartimento di Chimica Fisica "F. Accascina", Università degli Studi di Palermo, Viale delle Scienze, Parco D'Orleans II, 90128 Palermo, Italy

Received September 1, 2010. Revised Manuscript Received November 30, 2010

Dispersions of nanofillers into aqueous and solid biopolymeric matrices were studied from the physicochemical viewpoint. This work was carried out based on the idea that the combination of biopolymers, derived from renewable resources, and nanofiller, environmentally friendly, may form a new generation of nanomaterials with excellent and unique properties at low cost. To this purpose, two pectins with different degrees of methyl esterification and nanoclays like halloysite and laponite RD were selected. The thermodynamic and structural studies on the aqueous mixtures of pectin and nanoclay were able to discriminate the interactions, which control the adsorption of pectin onto the filler and the aggregation of both pectin and clay particles. The gained insights were useful to interpret the mesoscopic structure of the nanocomposites (prepared from the aqueous mixtures by means of the casting method) evidenced by SEM, thermal stability, tensile properties, and transparency investigations. The attained knowledge represents a basic point for designing new hybrid nanostructures in both the aqueous and the solid phase for specific purposes.

Introduction

The potential applications of biomaterials are numerous and involve different fields such as fibers for the textile industry, medical products, cosmetics, bioimplant, delivery of drugs, herbicides, fungicides, and so on.

On one side, one may consider the several biopolymeric materials (collagen, gelatin, chitosan, chitin, cellulose, starch, pectin, etc.). Films based on pectin and additives (such as poly(vinyl alcohol), chitosan, etc.) can be potentially used as water-soluble pouches for detergents, softeners, and medical delivery.[1] Pectin blended with high amylase starch and glycerol generates edible films with a large interval of mechanical properties[2] and excellent oxygen barrier capability.[3] Pectin−protein composite films may be used in wrapping and packaging materials in cases where moderate mechanical strength and low water vapor transmission are required.[4]

On the other side, nanoclays may be viable and inexpensive containers for various species.[5−7] Halloysite nanotube (HNT) is a green[7−10] filler, and being a natural product, its use does not add any risk to the environment as other nanofillers potentially do and it is also nontoxic.[11] The HNT external surface is composed of Si−O−Si groups, whereas the internal surface consists of a gibbsite-like array of Al−OH groups.[7] The combination of biopolymers and nanofillers may generate new materials with excellent and unique properties matching the great advantage to be composed of macromolecules, derived from renewable resources,[1,4] and nanoparticles, environmentally friendly—both components being available at low cost.

Within this issue, we thought it would be interesting to perform a physicochemical study on the aqueous mixtures of pectin and nanoclay with respect to their basic macroscopic, structural, and thermodynamic properties in dependence of the composition of both the polymer (pectins with two degrees of methyl esterification) and the filler (halloysite and laponite RD). The thermodynamic properties are suitable for evidencing the forces controlling the distribution of the nanofiller into the aqueous polymer matrix. The dynamic light scattering technique is sensitive to the filler/polymer mesostructures through their diffusion behavior. The determined macroscopic properties may be therefore correlated to the mesoscopic structure of the nanocomposites (prepared from the aqueous mixtures by using the casting method) evidenced by SEM, thermal stability, tensile properties, and transparency investigations.

In conclusion, this work was aimed at achieving deeper comprehension of pectin/nanoclay dispersions relevant for the design of new hybrid materials for rational purposes.

Experimental Section

Materials. Apple pectin (HM pectin, degree of methyl esterification, 74%, $M_w = 30-100$ kg mol^{-1}) and citrus pectin (LM pectin, degree of methyl esterification, 24%, $M_w = 30-100$ kg mol^{-1}), halloysite nanotubes ($Al_2Si_2O_5(OH)_4 \cdot 2H_2O$, HNTs), kaolinite, KBr, and KCl (≥99%) are from Aldrich. Laponite RD ($Na_{0.7}{}^{+}[(Si_8Mg_{5.5}Li_{0.3})O_{20}(OH)_4]^{0.7-}$) is a Rockwood product. All the materials were used without further purification. Water from reverse osmosis (Elga model Option 3) with a specific resistivity greater than 1 MΩ cm was used.

Preparation of Dispersions. We prepared a 2 wt % aqueous pectin solution under stirring at 70 °C. Then, an appropriate amount of nanofiller (laponite RD or HNT) was added to the pectin solution.

*Corresponding author. E-mail: g.lazzara@unipa.it.

(1) Tharanathan, R. *Trends Food Sci. Technol.* **2003**, *14*, 71–78.
(2) Coffin, D. R.; Fishman, M. L.; Ly, T. V. *J. Appl. Polym. Sci.* **1996**, *61*, 71–79.
(3) Coffin, D. R.; Fishman, M. L. *J. Appl. Polym. Sci.* **1994**, *54*, 1311–1320.
(4) Hassan-Nejad, M.; Ganster, J.; Bohn, A.; Pinnow, M.; Volkert, B. *Macromol. Symp.* **2009**, *280*, 123–129.
(5) De Lisi, R.; Lazzara, G.; Lombardo, R.; Milioto, S.; Muratore, N.; Turco Liveri, M. L. *Phys. Chem. Chem. Phys.* **2005**, *7*, 3994–4001.
(6) Viseras, M. T.; Aguzzi, C.; Cerezo, P.; Cultrone, G.; Viseras, C. *J. Microencapsulation* **2009**, *26*, 279–286.
(7) Lvov, Y. M.; Shchukin, D. G.; Möhwald, H.; Price, R. R. *ACS Nano* **2008**, *2*, 814–820.
(8) Fix, D.; Andreeva, D. V.; Lvov, Y. M.; Shchukin, D. G.; Möhwald, H. *Adv. Funct. Mater.* **2009**, *19*, 1720–1727.
(9) Shchukin, D. G.; Sukhorukov, G. B.; Price, R. R.; Lvov, Y. M. *Small* **2005**, *1*, 510–513.
(10) Veerabadran, N. G.; Mongayt, D.; Torchilin, V.; Price, R. R.; Lvov, Y. M. *Macromol. Rapid Commun.* **2009**, *30*, 99–103.
(11) Vergaro, V.; Abdullayev, E.; Lvov, Y. M.; Zeitoun, A.; Cingolani, R.; Rinaldi, R.; Leporatti, S. *Biomacromolecules* **2010**, *11*, 820–826.

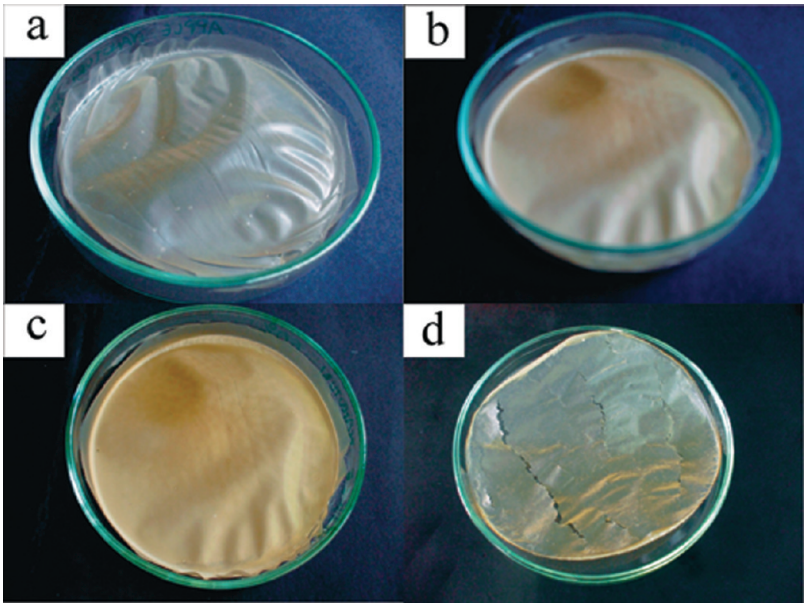

Figure 1. Films of nanocomposites formed by HM pectin and HNTs (a, C_f = 20 wt %; b, C_f = 60 wt %), kaolinite (c, C_f = 60 wt %), and laponite RD (d, C_f = 30 wt %). The diameter of the Petri dish is 9 cm.

For the density measurements, the nanofiller concentration was kept constant while the pectin composition was changed. In the case of laponite RD the ionic strength effect was also studied; namely, the pectin composition was maintained constant and the KCl concentration was changed.

For the preparation of nanocomposites formed by pectin and nanofiller, the well-dispersed aqueous mixture was poured into Petri dishes and heated at 80 °C for ~15 h to evaporate water. The films (with a thickness of ca. 0.06 mm) were easily removed from the supports and stored in a desiccator at room temperature. The composition of nanofillers (C_f) expressed as weight percent (grams of filler/100 g of nanocomposite) was systematically varied. In some cases the sample was prepared from a different batch of the aqueous dispersion, and the obtained composite shows reproducible behavior under thermal analysis investigation.

The prepared composites showed evident differences in the macroscopic aspect. The degree of methyl esterification does not play a role while the nanofiller nature does. The biocomposites based on HNTs and kaolinite exhibit compact mechanical features, and only for $C_f > 80$ wt % the material appears fragile. Examples for the HM pectin/nanofiller composites are reported in Figure 1. We therefore decided to carry out the experiments also on the composites rich in nanofillers. Laponite RD exercised a rather dissimilar effect (Figure 1) as the composites present a macroscopic structural deterioration at C_f = 20 wt %.

Methods. *Density*. The densities (±3 ppm) of the mixtures were determined at 25 and 35 °C by using a vibrating tube flow densimeter (Model 03D, Sodev Inc.). A closed loop temperature controller (Model CT-L, Sodev Inc.) maintained the temperature within 0.001 °C. The densimeter was calibrated according to the procedure described elsewhere.[12]

The specific volume of pectin in water was calculated as

$$v_{sp,M} = \frac{1}{d} - \frac{10^2(d - d_w)}{C_{p,w} d d_w} \quad (1)$$

where d and d_w are the densities of the aqueous pectin solution and water, respectively, while $C_{p,w}$ stands for the pectin concentration in water (weight percent).

The apparent molar volume ($V_{\Phi,f}$) of the nanofiller (laponite RD or HNTs) in a given mixture (pectin + water or KCl + pectin + water) was computed by means of the following equation

$$V_{\Phi,f} = \frac{M}{d} - \frac{10^3(d - d_0)}{m_f d d_0} \quad (2)$$

where m_f and M are the molality and the molecular mass of the nanofiller unitary cell, respectively (761.7 g mol^{-1} for laponite RD and 294.19 g mol^{-1} for HNTs); d and d_0 are the densities of the solution containing the nanoparticle and the corresponding solvent mixture, respectively. The nanofiller concentration was kept constant (ca. 6 mmol kg^{-1}). The measurements were performed on the mixtures just after their preparation (less than 2 h). The instability of the water + HNTs dispersion did not allow us to determine densities.

Dynamic Light Scattering. The measurements were performed at 18.0 ± 0.1 °C in a sealed cylindrical scattering cell at a scattering angle of 90° by means of a Brookhaven Instrument apparatus composed of an BI-9000AT correlator and a He−Ne laser (75 mW) with a wavelength (λ) of 632.8 nm. The solvent was filtered by means of a Millipore filter with 0.45 μm pore size.

Solutions of both pectins were investigated in a wide concentration domain. Afterward, dispersions of HNTs and laponite RD at variable concentration in the 0.1 wt % aqueous pectin solution were investigated.

For all of the systems, the field-time autocorrelation functions were well described by a monoexponential decay function (examples are illustrated in Figure 2), which provides the decay rate (Γ) correlated to the apparent diffusion coefficient (D)

$$D = \Gamma/q^2 \quad (3)$$

where $q = 4\pi n\lambda^{-1} \sin(\theta/2)$ is the scattering vector (n being the water refractive index and θ the scattering angle). The apparent hydrodynamic radius (R_h) was calculated by using the Stokes−Einstein equation and the water viscosity value.[13]

The dispersion of laponite RD in water did not provide reliable autocorrelation functions in the domain to 0.05 wt % due to low scattering intensity. This finding agrees with DLS results of

(12) De Lisi, R.; Lazzara, G.; Milioto, S.; Muratore, N. *J. Phys. Chem. B* **2003**, *107*, 13150–13157.

(13) *Handbook of Chemistry and Physics*, 89th ed.; Lide, D. R., Ed.; CRC Press: New York, 2008.

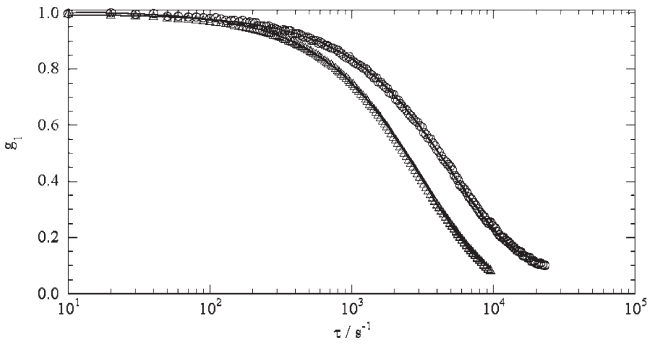

Figure 2. Field−time correlation functions of aqueous HM pectin 2 wt % in the absence (○) and the presence of HNTs $C_{f,w} = 0.011$ wt % (Δ). Lines are best fits according to the monoexponential decay.

laponite RD 0.5 wt %, which provided a small R_h value (22 nm).[14] Unfortunately, R_h of HNTs in water was not measured because the dispersions were unstable.

Thermogravimetry. The experiments were performed by means of a Q5000 IR apparatus (TA Instruments) under the nitrogen flow of 25 cm^3 min^{-1} for the sample and 10 cm^3 min^{-1} for the balance. The weight of each sample was ca. 15 mg. The measurements were conducted by heating the sample from room temperature to 900 °C with a rate of 10 °C min^{-1}. For each sample the following parameters were determined: the temperature of degradation (T_d), the percentage of moisture loss at 120 °C (ML_{120}), and the percentage of residual matter at 900 °C (RM_{900}). The ML_{120} and RM_{900} values were estimated from the dependence of the mass loss to temperature (TG curves), and the T_d values were taken at the maximum of the first-order derivative curves of mass loss to temperature (DTG curves). The TG experiments were also performed on some samples kept at room temperature and relative humidity of 70% for a few days.

Differential Scanning Calorimetry. The differential scanning calorimeter TA Instruments 2920 CE was used. The apparatus was calibrated with indium.[15] The measurements were carried out by heating and cooling the sample (ca. 5 mg) at 10 °C min^{-1} in the temperature range comprised between −10 and 300 °C.

Dynamic Mechanical Analysis. The DMA Q800 instrument (TA Instruments) was used to determine the mechanical properties from the stress−strain curves (some examples are reported in the Supporting Information). The samples were films of rectangular shape (10.00 × 6.00 × 0.060 mm^3). The stress ramp was set at 1 MPa min^{-1}. We determined the values of the elastic modulus (E), the tensile strength defined as the tensile stress at which the material fractures (σ_r), the percent elongation at break ($\varepsilon_{\%}$), and the yield strength (σ_y). Temperature was kept at 26.0 ± 0.5 °C.

Experiments were also carried out during heating at 4 °C min^{-1} from 100 to 250 °C, at the oscillation frequency of 1.0 Hz and strain amplitude of 0.05%.

Scanning Electron Microscopy. The morphology of nanocomposites was studied using a microscope ESEM FEI QUANTA 200F. Before each experiment, the surface of the sample was coated with gold in argon by means of an Edwards sputter coater S150A to avoid charging under electron beam. Minimal electron dose condition was set to avoid damage of the sample.

Films Transparency. The experiments were carried out at 25.0 ± 0.1 °C by using a Beckman spectrophotometer (model DU-640). Vis-absorption spectra were recorded as functions of λ from 400 to 800 nm. The attenuation coefficient (k) for each sample was computed as

$$k = A/(2.3D) \quad (4)$$

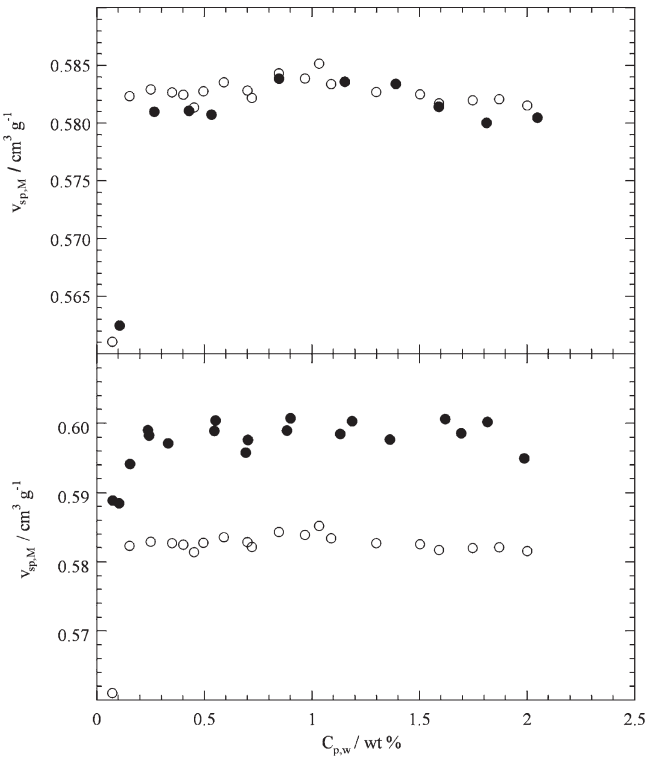

Figure 3. Dependence on pectin concentration of the specific volume of HM pectin (●) and LM pectin (○) in water at 25 °C (top) and LM pectin in water at 25 °C (○) and 35 °C (●) (bottom).

where A is the absorbance and D is the thickness of the rectangular film measured with a micrometer (±10^{-3} mm). The absorbance of nanocomposites with $C_f > 30$ wt % was not measured due to low transparency.

IR Spectroscopy. FT-IR spectra in KBr pellets were determined at room temperature in the spectral region 400−4200 cm^{-1} using a Perkin-Elmer (Spectrum BX) spectrometer. The spectral resolution is 2 cm^{-1}.

Results and Discussion

Aqueous Dispersions of Pectin/Nanofiller. *i. Pectins in Water*. As Figure 3 illustrates, $v_{sp,M}$ increases with $C_{p,w}$, reaching a nearly constant value, which does not depend on the pectin esterification degree. The $v_{sp,M}$ evidences the hydrophobic and Coulombic interactions as well as hydrogen bonds. The hydrophobic forces between the esterified groups are expected to be more relevant in the case of HM pectin. Electrostatic forces due to the pectins negative charges slightly contribute to $v_{sp,M}$; accordingly, data of LM pectin (0.5 wt %) reach a maximum reduction of 2% upon the addition of KCl (0.35 mol kg^{-1}) (see Supporting Information). A rather compact arrangement of the biomolecule with a low charge density may be adopted.[16] If, on one side, the hydrogen bonds generate a negative volume change,[17] on the other side, the formation of a close package should involve positive volume variations[18] as a consequence of desolvation phenomena. However, the degree of methyl esterification of the pectins does not play a relevant role on the dominant interactions.

Increasing temperature shifts the $v_{sp,M}$ vs $C_{p,w}$ trend in parallel toward larger values (Figure 3). The positive expansibility is

(14) De Lisi, R.; Lazzara, G.; Milioto, S.; Muratore, N. *Chemosphere* **2007**, *69*, 1703–1712.
(15) De Lisi, R.; Lazzara, G.; Milioto, S.; Muratore, N. *J. Therm. Anal. Calorim.* **2007**, *87*, 61–67.
(16) Kjøniksen, A.-L.; Hiorth, M.; Nyström, B. *Eur. Polym. J.* **2004**, *40*, 2427–2435.
(17) Lepori, L.; Gianni, P. *J. Solution Chem.* **2000**, *29*, 405–447.
(18) Tanford, C. *The Hydrophobic Effect: Formation of Micelles & Biological Membranes*, 2nd ed.; Wiley: New York, 1980.

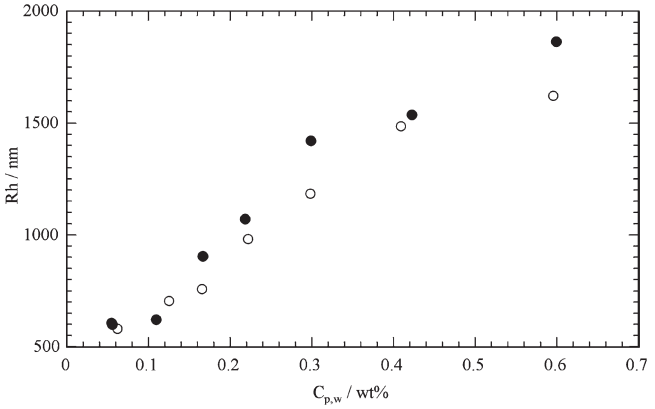

Figure 4. Apparent hydrodynamic radius of HM pectin (●) and LM pectin (○) in water as a function of the pectin concentration. The uncertainty of ±1% on the R_h values was estimated from the fitting procedure.

generated by the weakening of the inter- and intra-molecular interactions caused by the temperature raise.

The $v_{sp,M}$ data are consistent with the R_h dependence on $C_{p,w}$ for both LM and HM pectins in water. R_h is a measure of the diffusion coefficient of the scattering objects, and therefore its increase with $C_{p,w}$ (Figure 4) can be related to the occurrence of self-assembly controlled by hydrophobic association. On the other hand, the high R_h values agree with the presence of large aggregates. The degree of methyl esterification on R_h does not play a relevant role as on $v_{sp,M}$.

ii. Dispersed Nanofiller in Water + Pectin Mixtures. Figure 5 illustrates the trends of $V_{\Phi,f}$ as functions of $C_{p,w}$ for both the laponite RD/LM pectin and laponite RD/HM pectin systems at 25 °C. $V_{\Phi,f}$ decreases with $C_{p,w}$ to ca. 0.3 wt %; thereafter, it sharply increases reaching a maximum at ca. $C_{p,w}$ = 0.6 wt %. The peculiar dependence of $V_{\Phi,f}$ on $C_{p,w}$ may be explained in light of two phenomena: (1) the adsorption of the biomacromolecule onto the laponite RD surface and (2) the folding and compacting of the biomacromolecule at the solid/liquid interface. Furthermore, the sodium ions released by the nanodisks during the adsorption may favor the aggregation. For the mentioned phenomena $V_{\Phi,f}$ is expected to be negative and positive for processes 1 and 2, respectively; therefore, from a close inspection of graphs in Figure 5 one may assess that the dilute region (to $C_{p,w}$ = 0.3 wt %) is controlled by the adsorption while the intermediate region (0.3 wt % < $C_{p,w}$ < 0.6 wt %) by the aggregation. Being the data in the dilute region ($C_{p,w}$ < 0.3 wt %) not influenced by the degree of methyl esterification, one may deduce that the same adsorption process occurs for both pectins. For $C_{p,w}$ > 0.3 wt % the larger $V_{\Phi,f}$ in HM pectin may be ascribed to the bigger contribution of the hydrophobic aggregation at the interface.

The temperature does not play a role as data at 25 and 35 °C show (see Supporting Information). According to our description, both the adsorption and the aggregation processes are interconnected so that their variation as a consequence of temperature change are canceled out.

The ionic strength plays a peculiar role. $V_{\Phi,f}$ in water + KCl very strongly increases with KCl concentration (m_{KCl}) tending to a constant value (Table 1). By adding LM pectin 0.5 wt %, $V_{\Phi,f}$ is still an increasing function of m_{KCl} to ca. 0.15 mol kg^{-1}; thereafter, it decreases upon further addition of electrolyte (Table 1). The very sharp $V_{\Phi,f}$ variation (ca. 300 cm^3 mol^{-1}) in the absence of pectin agrees with the findings[19] that the ionic strength favors the aggregation of the clay platelets. In the presence of pectin, this process still takes place although it is reduced (the maximum increase is ca. 100 cm^3 mol^{-1}) by the pectin wrapping the nanodisks. Moreover, the pectin adsorption likely enhanced by the neutralization of the charges has to be considered, which explains the $V_{\Phi,f}$ decreasing values.

For HNTs/LM pectin at 25 °C $V_{\Phi,f}$ decreases in a wide $C_{p,w}$ range describing a minimum at ca. 0.7 wt % (Figure 5). This trend is still the combination of the two processes invoked to explain the laponite RD/LM pectin interactions. Under our experimental conditions (pH = 3.5), the HNTs[11,20] exhibit negative external

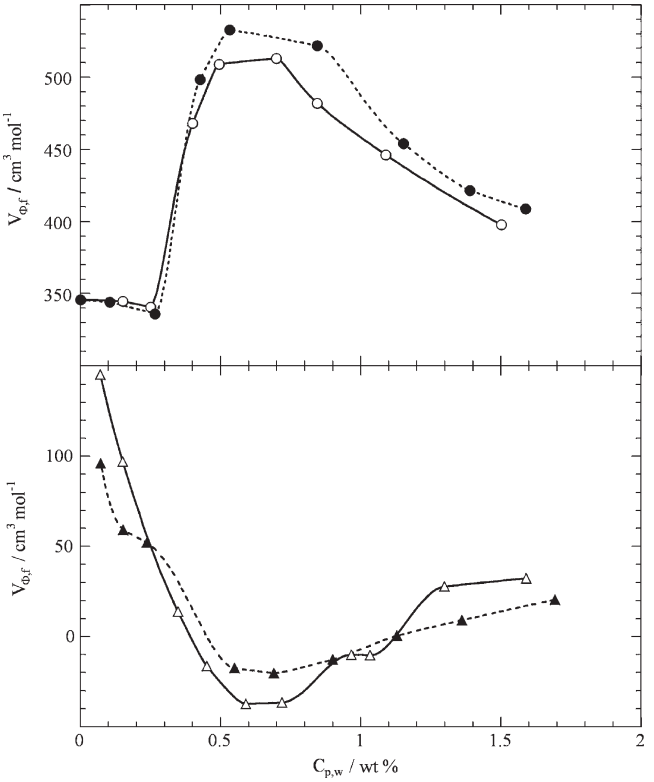

Figure 5. Apparent molar volume of nanoclays as functions of the biopolymer concentration for laponite RD/HM pectin at 25 °C (●), laponite RD/LM pectin at 25 °C (○), and HNTs/LM pectin at 25 (Δ) and 35 °C (▲). Lines are guide for eyes. The error is within the symbols being ±0.4 cm^3 mol^{-1}.

Table 1. Apparent Molar Volume of Laponite RD in Water + KCl and Water + LM Pectin 0.5% + KCl Mixtures[a]

m_{KCl}	$V_{\Phi,f}$
Water + KCl	
0	345.8
0.1439	656.3
0.3018	661.5
0.4991	643.0
Water + LM Pectin 0.5% + KCl	
0	508.9
0.0490	581.2
0.1613	597.3
0.3199	497.0
0.5002	412.3

[a] Units are m_{KCl}, mol kg^{-1}; $V_{\Phi,f}$, cm^3 mol^{-1}. The uncertainty on $V_{\Phi,f}$ is 0.3 cm^3 mol^{-1}.

(19) Nicolai, T.; Cocard, S. *Eur. Phys. J. E* **2001**, *5*, 221–227.

(20) Abdullayev, E.; Price, R.; Shchukin, D.; Lvov, Y. M. *ACS Appl. Mater. Interfaces* **2009**, *1*, 1437–1443.

Table 2. Apparent Hydrodynamic Radius for LM and HM Pectins in Water and in Aqueous Dispersions of HNT and Laponite RD[a]

LM pectin				HM pectin			
HNTs		laponite RD		HNTs		laponite RD	
$C_{f,w}$	R_h	$C_{f,w}$	R_h	$C_{f,w}$	R_h	$C_{f,w}$	R_h
0	504 ± 5	0	504 ± 5	0	784 ± 7	0	784 ± 7
0.013	520 ± 2	0.014	297 ± 2	0.011	574 ± 6	0.016	466 ± 4
0.021	567 ± 2	0.026	253 ± 5	0.021	560 ± 2	0.021	305 ± 4
0.036	550 ± 2	0.036	273 ± 5	0.034	586 ± 2	0.034	336 ± 4
0.040	534 ± 1	0.046	228 ± 4	0.049	435 ± 4	0.048	267 ± 3

[a] Units are $C_{f,w}$, wt %; R_h, nm. The errors on the R_h values were estimated from the fitting procedure.

surface and positive inner cavity. This means that, compared to laponite RD, HNTs present one more site of interaction with the biomacromolecule. The involved interactions are so strong that $V_{\Phi,f}$ assumes even negative values. Therefore, the sharp reduction of $V_{\Phi,f}$ with $C_{p,w}$ is an indication of the loading of COO^- groups into the lumen and the wrapping of the biomacromolecule onto the HNTs surface occurring via the ion-dipoles attractive forces. The increase of $V_{\Phi,f}$ reflects the predominance, over the adsorption, of the aggregation of LM pectin favored by the reduced charge density due to the low pH. The profile of $V_{\Phi,f}$ vs $C_{p,w}$ determined at 35 °C is similar to that at 25 °C, but oppositely to the findings for laponite RD/LM pectin system, temperature plays a role. At 35 °C, $V_{\Phi,f}$ decreases with a smaller slope than that at 25 °C, in agreement with some desorption of the biomacromolecule from the solid surface and with the consequent reduction of LM pectin aggregation.

As concerns the DLS data, all of the aqueous pectin/nanoparticle dispersions showed a single diffusion mode so that the diffusion of both the nanoparticle and the polymer was not discriminated. For a correct interpretation of DLS data, R_h of HNTs in water was estimated as[21]

$$R_h = \frac{L}{2\sigma - 0.19 - 8.24/\sigma + 12/\sigma^2} \quad (5)$$

being $\sigma = \ln(L/r)$, where r and L are the radius and the length of the nanotube. By introducing in eq 5 the average r and L values obtained from SEM data analysis (see below), the R_h value of 240 nm was computed. The absence of the diffusion coefficient for bare HNT in the aqueous pectin/HNT dispersions is proof of the polymer−nanotube interactions leading to a single diffusive mode ascribable to pectin-wrapped HNTs.

The decrease of R_h with $C_{f,w}$ for the laponite RD-based systems (Table 2) evidences that the nanofiller disturbs the pectin superstructure as a consequence of the adsorption of biomacromolecule onto the nanofiller surface as volume data highlighted. In the case of HNT based systems, R_h interpretation appears more complicated as in the presence of HM pectin R_h decreases while in the presence of LM pectin R_h slightly increases. The opposite trend may be ascribed to the dominant COO^-/HNTs lumen interactions for LM pectin, which favor the polymer networks formation.

Dried Dispersions of Pectin/Nanofiller: Bionanocomposites. Applying the nanotechnology to biopolymers represents a potential route for designing and producing new hybrid materials that, on one side, improves their properties (as several papers[22−24] on nanocomposites documented) and, on the other side, represents a challenge for an efficient cost-efficiency match.

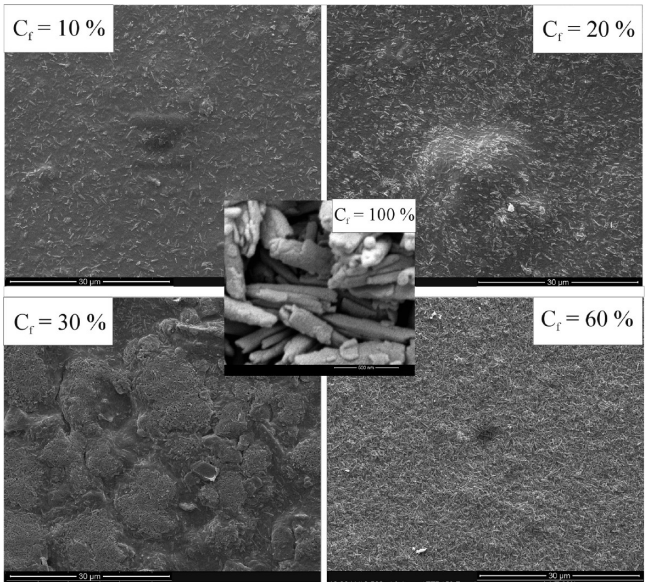

Figure 6. Scanning electron microscopy images for nanocomposites based on HM pectin and HNTs.

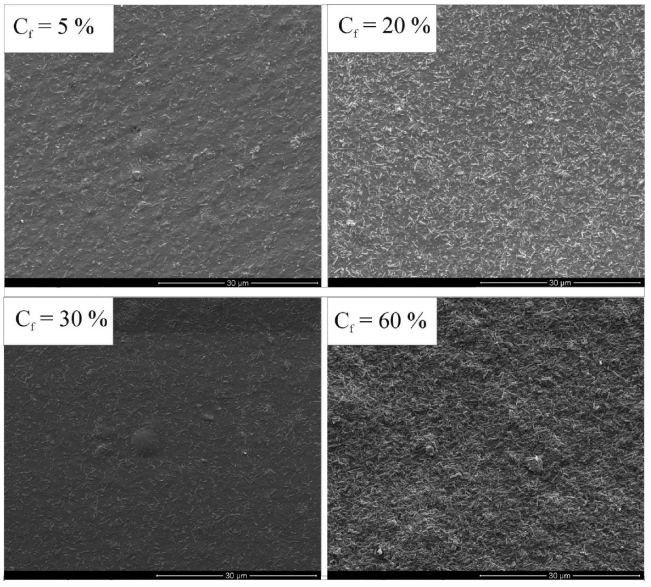

Figure 7. Scanning electron microscopy images for nanocomposites based on LM pectin and HNT.

Several routes may be followed to prepare nanocomposites. One of the most versatile is the melt blending procedure that, in our case, cannot be used because the polymer degradation takes place before the melting. We used the casting method, which requires that both the polymer and the filler are well dispersed into the solvent; that is the case here as the previous volume and DLS results demonstrated.

i. Microscopic Structure of Bionanocomposites. The morphology of nanocomposites, characterized by SEM (Figures 6 and 7), allows us to correlate the mesoscopic structure to the macroscopic properties. The peculiar structure of hollow tube with a spiral shape of HNTs is evident. A statistical analysis gave the average values of 73 ± 2 and 770 ± 20 nm for the radius and the length of the nanotube, respectively.

(21) Matsuoka, K.; Yonekawa, A.; Ishii, M.; Honda, C.; Endo, K.; Moroi, Y.; Abe, Y.; Tamura, T. *Colloid Polym. Sci.* **2006**, *285*, 323–330.
(22) Wang, X.; Du, Y.; Luo, J. *Nanotechnology* **2008**, *19*, 065707–0657013.
(23) Lazzara, G.; Milioto, S.; Gradzielski, M.; Prevost, S. *J. Phys. Chem. C* **2009**, *113*, 12213–12219.
(24) Sorrentino, A.; Gorrasi, G.; Vittoria, V. *Trends Food Sci. Technol.* **2007**, *18*, 84–95.

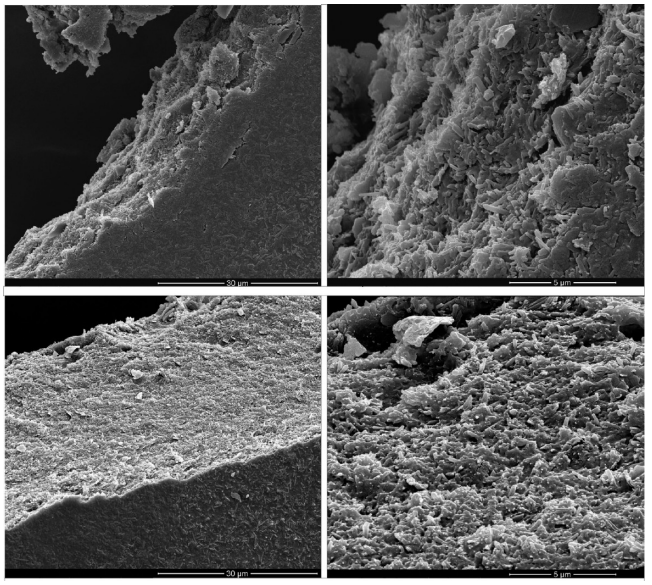

Figure 8. Scanning electron microscopy images of trasverse section for HM pectin/HNTs at C_f = 30 wt % (top) and LM pectin/HNTs at C_f = 20 wt % (bottom).

The micrographs of the HM pectin/HNTs and the LM pectin/HNTs systems show that the nanofiller is well dispersed into the polymer matrix and presents agglomerations only at very high filler compositions. We aforementioned that HNTs provide two sites of interaction with pectin, i.e., the external surface and the inner cavity. The forces between the nanotubes compete with the attractions between nanotube and pectin, which trigger the HNT-clusters formation. This phenomenon is retarded in LM pectin (C_f > 30 wt %) because the larger amount of carboxylic groups enhances interactions between the HNT and the pectin, rendering the system more uniform. This finding is consistent with DLS results. Figure 8 shows that, for both pectins, there is no stratification between the polymer and the nanotubes along with the thickness; thus, the filler is homogeneously dispersed through the edge of the nanocomposites.

The behavior of HNTs dispersed into the pectin matrix may be predicted through the percolation theory,[25] which was successfully applied to aqueous cylindrical micelles of a novel hydrogelator.[26]

In general, a system of independent nanoparticles of cylindrical shape dispersed in a continuous medium upon increasing the volume fraction (ϕ) generates a system controlled by nanoparticle−nanoparticle interactions. Such a transition takes place at the critical value ϕ_c calculated as[25]

$$1-\exp\left(-\frac{1.4[\pi r^2L+4\pi r^3/6]}{32\pi r^3/3+8\pi r^2L+\pi rL}\right)\leq\phi_c\leq 1-\exp\left(-\frac{2.8[\pi r^2L+4\pi r^3/6]}{32\pi r^3/3+8\pi r^2L+\pi rL}\right) \quad (6)$$

where r and L have the same meaning as above. For the pectin/HNTs systems, the ϕ_c value was calculated by introducing in eq 6 the values of r and L of the nanotubes provided by SEM results. Therefore, one obtains $0.082 \leq \phi_c \leq 0.16$, which corresponds to the C_f range between 11 and 21%.

Table 3. Parameters Obtained from the TGA Curves of Pristine Pectins[a]

	T_d	ML_{120}	RM_{900}
HM pectin	233.3	10.4	19.2
LM pectin	235.2	11.8	23.2

[a] Units are T_d, °C; ML_{120} and RM_{900}, wt %.

By further increasing ϕ, the nanoparticles are completely interconnected and the system becomes rigid at a ϕ_r value. For weakly interacting nanoparticles[25] $\phi_r = 4\phi_c$, and therefore we obtained $0.33 \leq \phi_r \leq 0.63$ (C_f from 41 to 70 wt %). It is relevant that such a theory predicts the microscopic behavior of the nanocomposites in a straightforward agreement with the experimental data. In fact, the micrographs in Figures 6 and 7 show that the HNTs are homogeneously dispersed for $C_f \leq 20$ wt % and form clusters for $C_f \geq 30$ wt %.

ii. Thermal Properties of Bionanocomposites. TGA is a valuable technique to characterize nanocomposites providing several works.[23,24,29,30] For a proper discussion of nanocomposites, TG curves of pristine components were determined. They show (Supporting Information) that both HM and LM pectins undergo a weight loss during heating from 25 to 120 °C and a further decrease at ca. 230 °C. The first weight loss is due to the moisture loss (ML_{120}) while the second one is generated by the degradation of the polymer. Between the two pectins, the LM pectin thermal stability is slightly enhanced (Table 3). The T_d values are comparable to those of other biodegradable polymers like cellulose[27] (T_d = 266 °C), poly(hydroxy butyrate−valerate)[28] (T_d =287 °C), and traditional plastics[29] (polypropylene with T_d = 295 °C and polystyrene with T_d = 270 °C).

DSC experiments on pectins did not evidence phase transitions but only an endothermic peak in the temperature range between 100 and 120 °C, which disappeared in the cooling curve. The area of the peak was combined with the enthalpy of water evaporation[31] (2259 J g^{-1}), and the water contents of 10.3 and 12.0% for the HM and LM pectins, respectively, were obtained. These values well agree with those from TGA studies (Table 3).

As concerns nanofillers (Supporting Information), the HNTs showed the weight loss of 12.7 and 5.7% at 465.7 and 717.5 °C, respectively, which were attributed to the expulsion of two water molecules of crystallization (theoretical value 12.2%) and to the subsequent loss of one water molecule (theoretical value 6.1%) produced by the dehydroxylation of alumina groups in agreement with the literature.[32] The kaolinite showed a loss of 10.2% at 535 °C due to one water molecule of crystallization. Laponite RD presents a ML_{120} value much higher (13.4%) than that of other fillers.

Figure 9 reports DTG examples on the influence of HNTs on the thermal stability of HM and LM pectins. The curves show that for the system based on HM pectin the peak temperature is shifted with the filler composition while for the system based on LM pectin the peak temperature hardly changes.

Figure 10 illustrates the degradation temperature (T_d) as a function of pectin concentration (C_p) for all the systems. The presence of very small amounts of nanofiller causes a thermal stabilization of HM pectin, which involves small changes (a few degrees) of the

(25) Celzard, A.; Pizzi, A.; Fierro, V. *J. Polym. Sci., Polym. Phys.* **2008**, *46*, 971–978.
(26) Buscemi, S.; Lazzara, G.; Milioto, S.; Palumbo Piccionello, A. *Langmuir* **2009**, *25*, 13368–13375.
(27) Nada, A. M. A.; Hassan, M. L. *Polym. Degrad. Stab.* **2000**, *67*, 111–115.
(28) Day, M.; Cooney, J. D. *J. Therm. Anal. Calorim.* **1998**, *52*, 261–274.
(29) Golebiewski, J.; Galeski, A. *Compos. Sci. Technol.* **2007**, *67*, 3442–3447.
(30) Lazzara, G.; Milioto, S. *Polym. Degrad. Stab.* **2010**, *95*, 610–617.
(31) D'Ans, L. In *Taschenbuch fur Chemiker und Physiker, Bd II*; Lax, E., Synowietz, C., Eds.; Springer-Verlag: Berlin, 1964.
(32) Yuan, W.; Jiang, G.; Che, J.; Qi, X.; Xu, R.; Chang, M. W.; Chen, Y.; Lim, S. Y.; Dai, J.; Chan-Park, M. B. *J. Phys. Chem. C* **2008**, *112*, 18754–18759.

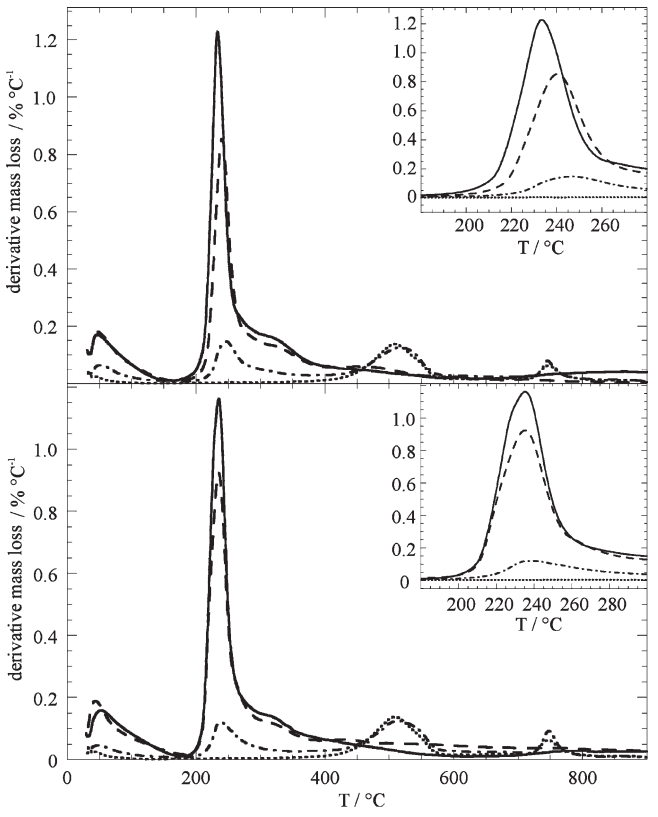

Figure 9. Thermal degradation rates as functions of temperature for the pectin/HNTs composites. (Top) HM pectin/HNTs: (···) pristine HNTs; (−·−) C_f = 80 wt %; (− −) C_f = 20 wt %; (—) pristine HM pectin. (Bottom) LM pectin/HNTs: (···) pristine HNTs; (−·−) C_f = 80 wt %; (− −) C_f = 15 wt %; (—) pristine LM pectin.

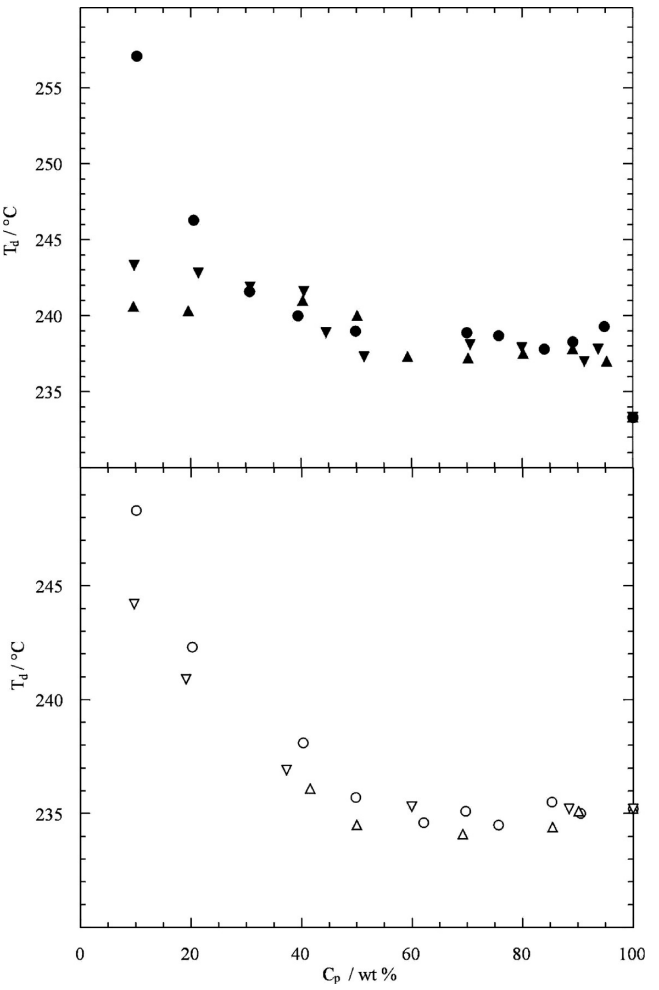

Figure 10. Degradation temperature as a function of pectin concentration for nanocomposites based on HM pectin (filled symbols) and LM pectin (open symbols) and HNTs (circle), laponite RD (triangle), and kaolinite (reverse triangle).

degradation temperature. A constant effect is registered to ca. 50 wt %; thereafter, T_d sharply rises with a slope specific of the nanofiller nature. Cellulose matrix reinforced with glycerol triacetate[9] and the thermoplastic starch with microfibers of cellulose increased the T_d values[33] as well as poly(methyl methacrylate) upon intercalation of montmorillonite.[34] In the case of LM pectin, T_d is not influenced by the presence of nanofiller to ca. 50 wt %, above which it sharply increases.

The dissimilarities in the thermal behavior of LM and HM pectins in the presence of the nanofiller can be straightforwardly interpreted in light of insights provided by the volume, DLS, and SEM studies. In the pectin domain (C_p to ca. 50 wt %) it was revealed that apart from the pectin adsorption on the nanofiller surface a concomitant aggregation of the biomacromolecule takes place, the latter being enhanced for HM pectin. Therefore, one may deduce that the more compact structure of the pectin becomes a sort of slight protection against the degradation, and it justifies the T_d few degrees larger than the value of pure HM pectin. The sharp increase of T_d in the dilute domain (C_p < 50 wt %) reveals significant thermal stability of pectin films generated as a consequence of the adsorption process. As a general result, for a given pectin, the HNTs exercise thermal stabilizing effect superior to that of laponite RD. The sharp enhancement of T_d may be ascribed to the pectin lodged into the HNT hollow, which is a good reservoir not only to protect the pectin but also to encapsulate the degradation products, delaying the mass transport. An entrapment mechanism of degraded products of poly(propylene) (PP) into the HNT lumens was invoked to explain the improvement of the PP/HNT nanocomposites thermal stability.[35] It appears that the lumens highly compensate for the loss of thermal stability induced by the HNTs clusters straightforwardly highlighted by SEM studies and percolation theory. Our explanation is corroborated by T_d of both HM and LM pectins in kaolinite, which presents similar chemical structure of HNTs but different morphological features; in fact, the flat kaolinite rolls into halloysite tubules.[7] For C_p < 50 wt % the T_d variation in the presence of kaolinite is less pronounced than that in HNTs, showing the key role of the tubular cavity. With the exception of composites based on laponite RD, for each system, ML_{120} is linearly correlated to C_f. The intercept and the slope values (see Supporting Information), independent of the polymer and the nanofiller nature, evidence the primary role of the water molecules in the polymeric matrix. These results are relevant in view of a quantitative determination of water content of nanocomposites provided that the impact of relative humidity on the films is taken into account. In our case, the exposure of the films for a few days at room temperature and relative humidity of 70% caused a water increase of 1%, which is lower than the uncertainty on ML_{120} value calculated from data reported in the Supporting Information.

(33) Averous, L.; Boquillon, N. *Carbohyd. Polym.* **2004**, *56*, 111–122.
(34) Gao, Z.; Xie, W.; Hwu, J. M.; Wells, L.; Pan, W. P. *J. Therm. Anal. Calorim.* **2001**, *64*, 467–475.
(35) Mingliang, D.; Baochun, G.; Demin, J. *Eur. Polym. J.* **2006**, *42*, 1362–1369.

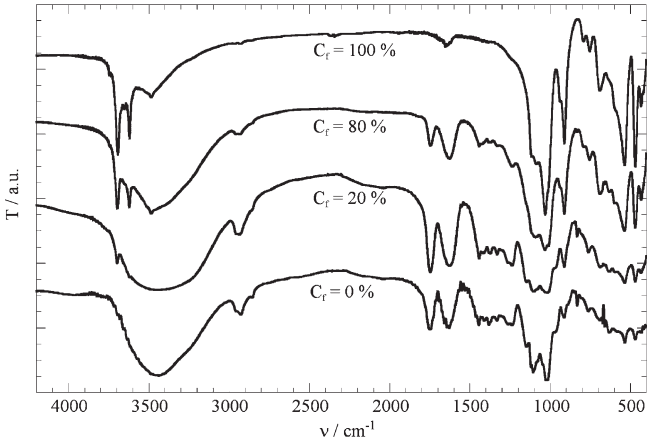

Figure 11. FTIR spectra of HM pectin, HNTs, and their nanocomposites.

We finally focus attention on the residual matter at 900 °C (RM_{900}), from which the weight percentage of nanocomposite degraded at that temperature (DM_{900}) may be calculated:

$$DM_{900} = 100 - (RM_{900} + ML_{120}) \quad (7)$$

Assuming that the pectin−filler interactions in the nanocomposites do not alter the residual matter at 900 °C of each component, DM_{900} is computed as

$$DM_{900} = 10^{-2} C_f (DMf_{900} - DMp_{900}) + DMp_{900} \quad (8)$$

where DMf_{900} and DMp_{900} correspond to the weight percentage of pure filler and pectin at 900 °C. Equation 8 predicts a linear correlation between DM_{900} and C_f. For all of the investigated systems, such a linearity was observed so that the intercept and the slope were determined (data are reported in the Supporting Information). These parameters agree very well with the values computed by using the experimental DMf_{900} and DMp_{900} of the pristine components. This approach was successful even for consolidated archaeological woods.[36] In conclusion, eq 8 is an excellent tool for a quantitative evaluation of the filler content in the nanocomposites with unknown composition.

iii. FTIR Spectroscopy for Bionanocomposites. The FTIR spectra of HM pectin, HNTs, and their nanocomposites are reported in Figure 11. The spectra of both pristine components are consistent with those reported in the literature.[37−39] The spectra of the systems at C_f = 20 and 80 wt % are rather similar to those of pure biopolymer and HNTs, respectively. In particular, the signals at 3697 and 3623 cm^{-1} attributed to the stretching vibrations of inner-surface OH groups of HNTs are well evident for the system at C_f = 80 wt %, and even at high HM pectin loading, one may observe the peak at 3697 cm^{-1}. The large band at 3440 cm^{-1} in the spectrum of pure LM pectin generated by the stretching of the OH groups (originated from both the macromolecule chemical structure and the hydration water molecules) is also present at C_f = 80 wt %. On the other hand, previous TG experiments detected water in the nanocomposites. The peak at 1644 cm^{-1} in the spectrum of pure HNT is due to the weak deformation vibration of the water in the interlayer. In the presence of HM pectin it disappears because of the concomitant presence of the peak at 1625 cm^{-1} due to the COO asymmetric bending of the biopolymer.

Table 4. Dynamic Mechanical Properties of Pure Pectins and Their Nanocomposites[a]

C_f	E	$\varepsilon_{\%}$	σ_y	σ_r
		HM Pectin/HNTs		
0	2103 ± 3	2.61 ± 0.02	20.8 ± 0.3	33.2 ± 0.5
21.20	1828 ± 8	3.75 ± 0.02	15.6 ± 0.3	29.0 ± 0.6
30.03	1731 ± 3	1.67 ± 0.02	14.7 ± 0.3	20.0 ± 0.4
60.59	3724 ± 9	1.15 ± 0.02	9.64 ± 0.09	20.6 ± 0.2
79.59	2601 ± 9	0.76 ± 0.02	6.54 ± 0.04	12.22 ± 0.08
		LM Pectin/HNTs		
0	2370 ± 4	4.29 ± 0.02	25.0 ± 0.5	41.6 ± 0.8
19.87	2182 ± 6	1.94 ± 0.02	17.5 ± 0.2	26.0 ± 0.4
29.80	2831 ± 5	3.12 ± 0.02	16.5 ± 0.3	34.0 ± 0.5
		HM Pectin/Laponite RD		
19.87	693 ± 4	2.30 ± 0.02	10.6 ± 0.1	13.6 ± 0.2

[a] Units are C_f, wt %; E, σ_y, and σ_r, MPa; ε%, %.

In conclusion, one may state that the HNT/HM pectin forces generate neither appreciable variations in the position of the peaks nor appearance of new vibrations which is consistent with the absence of new covalent bonds formation between the filler and the polymer in the nanocomposites.

iv. Tensile Properties of Bionanocomposites. The mechanical properties for pure pectins and nanocomposites based on HNTs are collected in Table 4. The performance of LM pectin is better than that of HM pectin ascribable to the presence of larger number of hydrogen bondings. The properties of films based on both pectins are superior to those of other biopolymers generally used to produce nanocomposites. For example, for thermoplastic starch[40] E = 111 MPa, σ_y = 4.4 MPa, and σ_r = 11.2 MPa. Moreover, they are rather similar to the dynamic mechanical properties of many traditional plastics used for packaging; poly(vinyl acetate)[41] presents E values ranging between 1275 and 2256 MPa and σ_r values between 29 and 49 MPa.

The presence of HNTs (C_f = 20 and 30 wt %) causes a slight deterioration in the mechanical performance of both pectins with the exception of the elongation at break of HM pectin/HNT (C_f = 20 wt %). These results are rather unusual, but they are not unique as, for instance, the multiwalled carbon nanotubes improved both E and σ_y but deteriorated $\varepsilon_{\%}$ of chitosan.[42]

Very intriguing appear the properties at high HNTs loading. The elastic modulus of pectins reinforced with HNTs is substantially increased (the elasticity of the HM pectin/HNTs film at C_f = 60 wt % is presented in a short video in the Supporting Information); for these compositions a sharp enhancement of thermal stability was found (Figure 10). On the other hand, the $\varepsilon_{\%}$, σ_y, and σ_r parameters still decrease their values. The HNTs generated an improvement of tensile strength and elongation at break of ethylene propylene diene monomer even at high composition.[43] Moreover, HNTs (few percent) in industrial oil-based paint generated an improvement of the tensile properties.[20] Tensile tests carried out on the HM pectin/laponite RD (C_f = 20 wt %)

(36) Donato, D. I.; Lazzara, G.; Milioto, S. *J. Therm. Anal. Calorim.* **2010**, *101*, 1085–1091.
(37) Luo, P.; Zhao, Y.; Zhang, B.; Liu, J.; Yang, Y.; Liu, J. *Water Res.* **2010**, *44*, 1489–1497.
(38) Yuan, P.; Southon, P. D.; Liu, Z.; Green, M. E. R.; Hook, J. M.; Antill, S. J.; Kepert, C. J. *J. Phys. Chem. C* **2008**, *112*, 15742–15751.
(39) Winning, H.; Viereck, N.; Salomonsen, T.; Larsen, J.; Engelsen, S. B. *Carbohydr. Res.* **2009**, *344*, 1833–1841.
(40) Alemdar, A.; Sain, M. *Compos. Sci. Technol.* **2008**, *68*, 557–565.
(41) *Polymer Data Handbook*; Mark, J. E., Ed.; Oxford University Press: New York, 1999.
(42) Wang, S. F.; Shen, L.; Zhang, W. D.; Tong, Y. J. *Biomacromolecules* **2005**, *6*, 3067–3072.
(43) Ismail, H.; Pooria, P.; Ahmad, F. M. N.; Abu Bakar, A. *Polym. Test.* **2008**, *27*, 841–850.

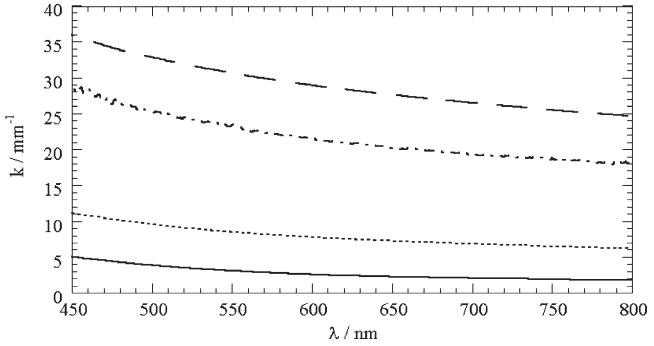

Figure 12. Dependence of the attenuation coefficient on the wavelength for the HM pectin/HNTs nanocomposites at $C_f = 0$ (—), 10 (---), 25 (−·−), and 30 (——) wt %.

showed a significant worsening of the mechanical properties (Table 4).

The dynamic mechanical tests under oscillatory regime were performed because the loss tangent (tan δ) of the material (Supporting Information) is indicative of structural changes and phase transitions. In the case of clay nanocomposites, the tan δ increase was ascribed to the three-dimensional interconnecting network of filler layers.[41] The loss tangent as a function of temperature measured for HM pectin/HNTs ($C_f = 20$ and 60 wt %) is independent of temperature to around 200 °C; thereafter it increases. The break is generated by the degradation of HM pectin. In fact, the temperature values at the onset of the tan δ vs temperature trend (219.9 and 226.5 °C for $C_f = 20$ and 60 wt %, respectively) agree with those from TG curves (221.2 and 224.6 °C for $C_f = 20$ and 60 wt %, respectively).

As a general result, the pectin/HNT nanocomposites exhibit dynamic mechanical properties competitive with those of many traditional plastics[41] and interestingly do not suffer any structural change as a consequence of temperature raise.

v. Films Transparency of Bionanocomposites. Examples of the dependence of the attenuation coefficient (k) on λ for the HM pectin/HNT nanocomposites are shown in Figure 12 (k data of other systems are in the Supporting Information). For all of the systems one observes a larger k value at lower λ. By adding HNTs to pectin shifts in parallel, the k vs λ trends toward higher values.

The phenomenon of light scattering is certainly influenced by the morphology of the filler, the tendency to form aggregates, and the filler concentration. Computation of k values based on the size and the concentration of anisotropic particles and polydispersity is rather complicated. For spherical particles it is reported[44] that $k \propto \phi R$, where R is the radius of the spherical particles scattering light while ϕ is their volume fraction so that the k vs ϕ slope is proportional to R. To apply this model to our systems (Figure 13), k at the arbitrary λ value of 750 nm was chosen (k_{750}). Being that the particles do not have a spherical shape, R assumes a more general meaning that is an apparent radius of spherical particles having the same scattering property of the real particles. The ϕ values for each system were calculated by using the densities for pectin,[34] HNTs,[7] kaolinite,[45] and laponite RD.[46]

In the case of HM pectin/HNTs system (Figure 13), the linear trend of k vs ϕ in the domain to $\phi = 0.10$ (which corresponds to

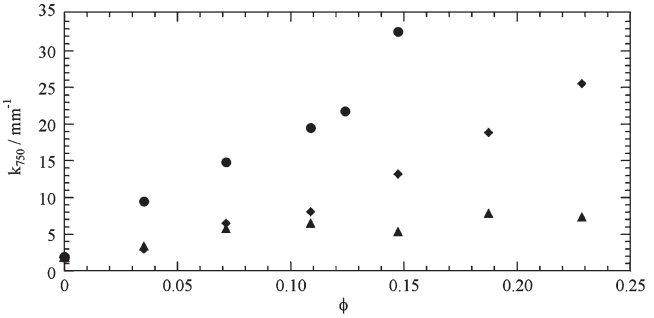

Figure 13. Dependence of the attenuation coefficient at 750 nm on the filler volume fraction for HM pectin mixed with HNTs (◆), laponite RD (▲), and kaolinite (●).

$C_f = 20$ wt %) indicates that the individual particles do not form aggregates. The deviation from linearity occurring at higher concentrations reflects the organization into clusters of nanotubes (wrapped by the adsorbed pectin) with apparent radii progressively increasing upon the filler addition. These results are in a very good agreement with the microscopic structure evidenced by SEM experiments. Kaolinite and laponite RD (Figure 13) show the largest and the smallest slopes, respectively, in agreement with the particle size. Similar findings are obtained for the nanocomposite formed by LM pectin.

In conclusion, the films transparency may be modulated by changing either the composition or the filler size.

Conclusions

Hybrid films composed of biomass sourced polymers and clays were examined. The aqueous mixture used to prepare these materials showed that pectins wrap the nanoclays, allowing the formation of stable dispersions. Laponite RD exhibits one site of interaction, while HNT does two sites, i.e., the outer surface and the lumen. The large number of $-COO^-$ groups in LM pectin interact with the HNTs lumen, favoring the polymer network formation in aqueous solution. The opposite result is obtained for the laponite RD.

SEM micrographs evidenced that HNTs are well dispersed in the polymer matrix up to a given concentration, above which they form clusters in agreement with the percolation theory. The HNT-based nanocomposites exhibit mechanical properties competitive with those of many traditional plastics even at high filler loading and do not suffer any structural change due to the temperature raise. Moreover, the presence of biopolymer on the surface and into the lumen generates a sharp enhancement of the thermal stability and elastic modulus in the case of high nanoclay loading where clusters are present. The transparency of films may be finely tuned as lower loading and a small sized filler confer larger light transparency. On the basis of TGA experiments, a protocol for a quantitative estimation of the filler, if unknown, and water content in the nanocomposites was proposed.

Acknowledgment. The work was financially supported by the University of Palermo and COFIN 2008 " Preparazione e caratterizzazione chimico-fisica di nanocompositi funzionali a mattoni innovativi in terra cruda" (Prot. 2008RH3FCW_002). We thank the "Fondazione Banco di Sicilia" (Palermo, Italy), which cofinanced the TGA Q5000 IR apparatus (Convenzione PR 4.b/08), and TA Instruments, Italy (Vimodrone-MI), for supporting us in the DMA experiments. Prof. V. Turco Liveri and Dr. A. Ruggirello are also acknowledged for allowing us to perform FTIR experiments.

(44) Pogodina, N. V.; Cerclé, C.; Avérous, L.; Thomann, R.; Bouquey, M.; Muller, R. *Rheol. Acta* **2008**, *47*, 543–553.
(45) Katz, H. S.; Milewski, J. V. *Handbook of Fillers for Plastics*; Van Norstrand-Reinhold: New York, 1987.
(46) Nelson, A.; Cosgrove, T. *Langmuir* **2004**, *20*, 2298–2304.

Supporting Information Available: Video showing the nanocomposite elasticity; stress/strain curves for nanocomposites; loss tangent as a function of temperature for HM pectin/HNTs; TG curves of pristine pectins and nanofillers; DSC thermograms of pectins; attenuation coefficient for LM pectin-based systems; apparent molar volume of laponite RD as functions of the LM pectin concentration at 35 °C; tables of experimental density data; calculated and experimental intercept and slope of eq 8; experimental intercept and slope for the dependence of ML_{120} on the filler concentration. This material is available free of charge via the Internet at http://pubs.acs.org.